VLSI Implementation of Chest X-Ray Image Segmentation Using Hybrid Clustering

G. Suresh[1], Gottam Meghana[1], Esanaka Naga Sujitha[1], Isanaka Deekshitha[1], Guduru Kundana Priya[1]

[1]Department of Electronics and Communication Engineering, Geethanjali Institute of Science and Technology, Nellore.

Abstract: Medical image segmentation plays a crucial role in various clinical applications, facilitating accurate diagnosis and treatment planning. In communication systems, particularly telemedicine and remote healthcare monitoring, real-time processing and transmission of medical images are essential for timely diagnosis and intervention. Leveraging VLSI technology for implementing K-means offers a promising solution to address the computational demands of image segmentation while meeting the stringent requirements of communication systems. Existing systems often rely on software-based implementations such as threshold segmentation, leading to significant computational overhead and latency, particularly in resource-constrained environments. Moreover, these implementations struggle to achieve real-time performance, hindering their practical utility in communication systems for healthcare. So, this work proposed VLSI-based approach aims to overcome these challenges by offloading the computational burden from the software to hardware, enabling parallel processing and efficient utilization of resources. By exploiting the inherent parallelism of the K-means algorithm and optimizing hardware architecture, our design ensures high throughput and low latency, making it suitable for real-time medical image segmentation in communication systems.

Keywords: Hybrid Clustering, Image Segmentation, Pixel Analysis, Chest x ray images, Xilinx.

1. Introduction

At present, this technology has made some progress in chest disease diagnosis. However, artificial intelligence-based diagnosis technique still has many obvious drawbacks. For example, these include low-level feature recognition, small proportion of disease spots, and changeable disease location between the chest disease and the remaining normal area, compared with those from real images, due to the coarse-grained recognition [1]. Therefore, it is hard to make connections between features, and finding the subtle traits that fully characterize the object is not straightforward, so the fine-grained classification of chest diseases is very challenging due to the difficulty of finding discriminative features [2]. It is also difficult to find the most representative features for fine-grained classification of chest diseases. On the other hand, the imbalance between normal and disease X-ray images makes it challenging to design accurate diagnostic algorithms. This can lead to misdiagnosis, as the gradient direction tends to favor normal X-ray images [3]. Current algorithms can only detect whether an image is diseased or not but have difficulty identifying the specific type of disease and differences between them. To conquer those problems, binary cross-entropy is used in this study to balance the number of disease and normal X-ray images and compensate for the loss function among graph mining techniques for imaging classification, clustering algorithms are extraordinarily critical, since they can categorize objects into different groups according to their similarities. Traditional clustering algorithms [4,5], such as K-means [6], are limited by their spherical assumptions, which can lead to local optima. Spectral clustering [7] has rapidly developed in recent years to compensate for these limitations by leveraging the eigenvalues of the similarity matrix. Fiedler initialized spectral clustering algorithm, unlike traditional clustering algorithms, spectral clustering does not rely on shape assumptions and can find the global optimum. It has been widely used in VLSI design [8], load balancing, parallel computing [9], and sparse matrix partitioning. Spectral clustering is advantageous in both theoretical and practical applications, and it can be applied to any distribution pattern without considering dependency assumptions.

2.Literature Survey

Jyoti, Kumari, et.al [10] proposed the TQWT parameters optimized for PSNR and SSIM yielded promising results. MCA-based model enabled efficient storage and classification using ResNet50 and Alex Net CNN models, achieving average accuracies of 98.82% and 94.64% for small and large datasets, respectively, surpassing conventional deep learning methods. Sulaiman, Adel, et.al [11] developed COVID-19 and tuberculosis are prevalent lung diseases, yet joint diagnosis approaches are limited. A proposed deep learning model detects these diseases from chest X-ray images, achieving 98.72% accuracy across all classes. With a recall score of 99.66% for Pneumonia, 99.35% for No-findings, 98.10% for Tuberculosis, and 96.27% for COVID-19, it outperforms existing studies. Nayak, Soumya Ranjan, et.al [12] developed the COVID-19 epidemic spurred intensive AI-based studies, but heavy models posed time and memory constraints. A lightweight CNN approach was devised for multi-class and binary classification of chest X-rays, achieving 98.33% accuracy.

Priya, R. Krishna, et.al [13] developed the storage and processing of medical data irrespective of the physical location of lab are explored in this research with Cloud computing. Extracted valid information from a medical image was high importance in the medical arena. The information loss may lead to the misinterpretation of medical image analysis and treatment analysis. Nawaz, Marriam, et.al [14] developed the competence of machine learning approaches to carry out clinical expertise tasks has recently gained a lot of attention, particularly in the field of medical-imaging examination.

Among the most frequently used clinical-imaging modalities in the healthcare profession is chest radiography. Shaheed, Kashif, et.al [15] developed the COVID-19 tests quickly, accurately, and consistently. Methods: Using chest X-ray images, this study proposed a cutting-edge scheme for the automatic recognition of COVID-19 and pneumonia.

Arvind, S., et.al [16] developed the Deep models had immensely contributed to this sector thus making it easier for quick diagnosis, early and effective treatment. X-Rays are the most used radiological medical imaging tool and radiologists. Medical practitioners face huge difficulty classifying and segmenting different organs by looking at the chest X-Rays. Rajaraman, Sivaramakrishnan, et.al [17] developed the Deep learning (DL) models was state-of-the-art in segmenting anatomical and disease regions of interest (ROIs) in medical images. Particularly, many DL-based techniques have been reported using chest X-rays (CXRs). dos Santos Silva, Bruno Riccelli, et.al [18] developed the time necessary to confirmed patient infection can be lengthy, and the process was expensive. On the other hand, X-Ray and CT scans play a vital role in the auxiliary diagnosis process. Hence, a trusted automated technique for identifying and quantifying the infected lung regions would be advantageous. Rollan-Martinez-Herrera, Maria, et.al [19] developed the thorax segmentation approach in Chest Radiographs based on a U-Net architecture that captures useful information from the mediastinal region, which was often discarded in lung-based segmentation. Farhan, Abobaker Mohammed Qasem, et.al [20] developed the chest X-ray images provided vital information about the congestion cost-effectively. They proposed a novel Hybrid Deep Learning Algorithm (HDLA) framework for automatic lung disease classification from chest X-ray images.

3. Proposed Methodology

Figure 1 proposed system architecture, which illustrates a process starting with the input of a chest X-ray image, followed by its reading into MATLAB for further analysis. Once the image is imported, MATLAB performs preprocessing tasks to enhance its quality and reduce noise. Subsequently, the preprocessed image undergoes conversion into text format within MATLAB. This step involves extracting relevant features or characteristics from the image and representing them as text data, potentially aiding in further computational analysis or integration with other systems. The text data obtained from the previous step is then input into a hybrid clustering algorithm implemented in VLSI. Hybrid clustering combines multiple clustering techniques to achieve more accurate and efficient segmentation. Once clustering is performed, the resulting segmented text data is output from the VLSI system. Following this, MATLAB takes over again by converting the segmented text data back into an image format, reconstructing the segmented regions based on the clustering results. Finally, the output of this process is the segmented chest X-ray image, where different anatomical structures or abnormalities are delineated, potentially aiding medical professionals in diagnosis and treatment planning.

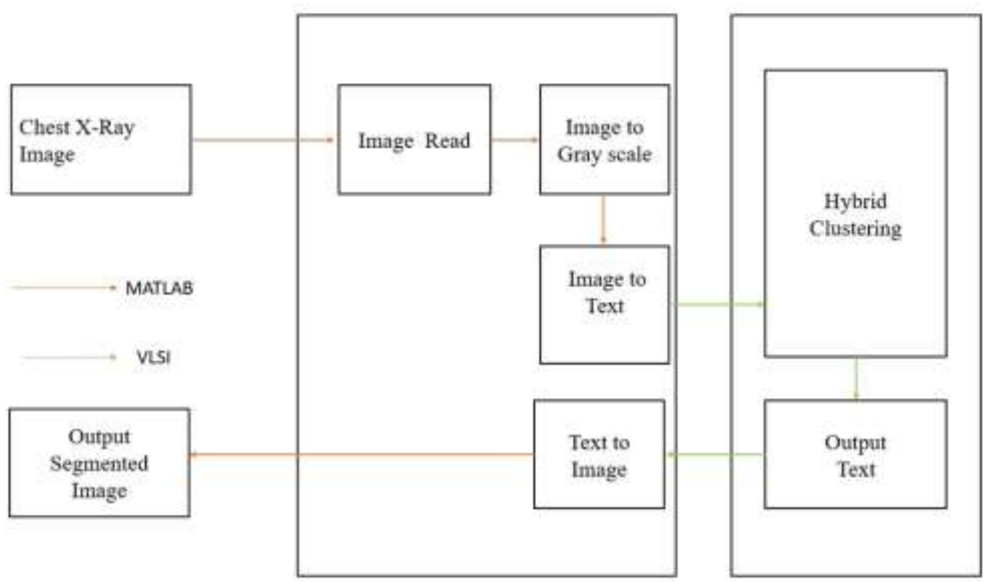

Figure 1. Proposed block diagram

3.1 VLSI Based Hybrid Clustering Process

Step-1: Read the input pixels data and store them into memory: In the first step of a hybrid clustering approach, the input pixels data are read and stored into memory. This process involves retrieving the pixel values from the source, which could be an image file, a database, or any other data repository containing the pixel information. The pixel data typically include attributes such as color values (e.g., RGB or grayscale intensity), spatial coordinates, or other relevant features depending on the specific application. These pixel values are then loaded into memory, usually in the form of arrays or matrices, to facilitate subsequent processing. The algorithm begins by reading the input image data and storing it into the computer's memory. This process involves loading the image pixel by pixel, where each pixel typically contains information about its color or intensity. By storing the pixel data in memory, the algorithm gains access to the raw image information, enabling further processing to identify and segment different regions or individuals within the image.

Step-2: Automated No of Clusters Selection: In the second step of hybrid clustering, the algorithm focuses on automatically determining the optimal number of clusters to be created based on the characteristics of the input image data. This is a crucial step as it ensures the segmentation process is adaptive and tailored to the specific complexities and variations present in human images. Various techniques can be employed to automatically select the number of clusters, such as statistical methods, density-based approaches, or heuristics based on image properties like texture, color distribution, or edge detection.

Step-3: Cluster Analysis with cluster-to-cluster similarity measurement: In the third step of hybrid clustering, the algorithm performs cluster analysis on the pixel data to identify distinct groups or clusters that represent different parts of the image. This involves applying clustering techniques such as k-means, hierarchical clustering, or density-based clustering to partition the pixels into cohesive groups based on their similarities in color, texture, or other features. Additionally, the algorithm evaluates the similarity between clusters to understand how different regions or individuals in the image relate to each other spatially and visually.

Step-4: Internal Cluster Values Analysis With pixel-to-pixel difference estimation: In the fourth step of hybrid clustering, the algorithm focuses on analyzing the internal values of each cluster and assessing whether there are significant differences between pixel values within clusters. By examining the internal characteristics of clusters, such as the distribution of pixel intensities or color values, the algorithm gains insights into the homogeneity or coherence of each cluster. This analysis helps ensure that each cluster represents a distinct and coherent region or individual within the image, enhancing the accuracy and reliability of the segmentation results.

Step-5: Resultant Two Clusters Generation: In the fifth step of hybrid clustering, the algorithm finalizes the clustering process by reducing the number of clusters to a predefined quantity, such as two clusters for binary segmentation representing foreground and background. This reduction is often achieved through cluster elimination or merging similar clusters. The goal is to simplify the segmentation while preserving the essential features and details of the image. By maintaining a smaller number of clusters, the segmentation result becomes more interpretable and easier to analyze.

Step-6: Maximum pixel values Based regions finalization: In the sixth step of hybrid clustering, the algorithm focuses on maintaining maximum pixel values for color difference. This involves adjusting the cluster centroids or boundaries to ensure that the color differences between clusters are maximized, thereby enhancing the visual distinction between different segments of the image. The hybrid clustering algorithm iteratively refines the segmentation process by iteratively considering the maximum pixel values within each cluster to delineate regions. By focusing on the most intense or salient areas within each cluster, the algorithm can effectively separate distinct objects or features within the image, even in cases where there may be overlapping or ambiguous boundaries. This finalization step plays a crucial role in improving the segmentation quality by ensuring that regions are accurately delineated based on their dominant visual characteristics, ultimately contributing to more precise and meaningful image analysis and interpretation. By optimizing the color differences between clusters, the algorithm aims to improve the clarity and accuracy of the segmentation result, making it easier to discern between different regions such as disease effected or normal within the image.

Step-7: Generate output text file: In the seventh step of hybrid clustering, the algorithm generates an output text file containing the segmented regions or individuals. This text file typically includes information about the location, size, and characteristics of each segment, allowing for easy access and interpretation of the segmentation results. By storing the segmentation output in a text format, the algorithm enables further analysis or processing of the segmented image data using various software tools or programming languages.

4.Results and Discussions

Figure 2 illustrates the simulation outcome, which presumably showcases the results of running the segmentation algorithm on a dataset. Figure 3 presents a design summary, likely detailing the architecture or methodology of the segmentation algorithm. Figure 4 offers a power summary, which could refer to computational power consumption or efficiency metrics of the segmentation algorithm. Figure 5 depicts a time summary, likely showcasing the time-related metrics of the segmentation algorithm, such as processing time per image or overall runtime. Figure 6 is split into two parts, illustrating the performance of the segmentation algorithm through segmented images. Part (a) shows an input image, while part (b) displays the segmented output image generated by the proposed method. This comparison visually demonstrates the effectiveness of the algorithm in accurately segmenting objects or regions of interest within the images.

Table 1 provides a detailed comparison between the existing segmentation method and the proposed method across various performance metrics, including accuracy, sensitivity, F-measure, precision, Matthew's correlation coefficient (MCC), Dice coefficient, Jaccard coefficient, and specificity. The proposed method significantly outperforms the existing method across all metrics, indicating its superiority in accurately delineating objects or regions of interest in the images.

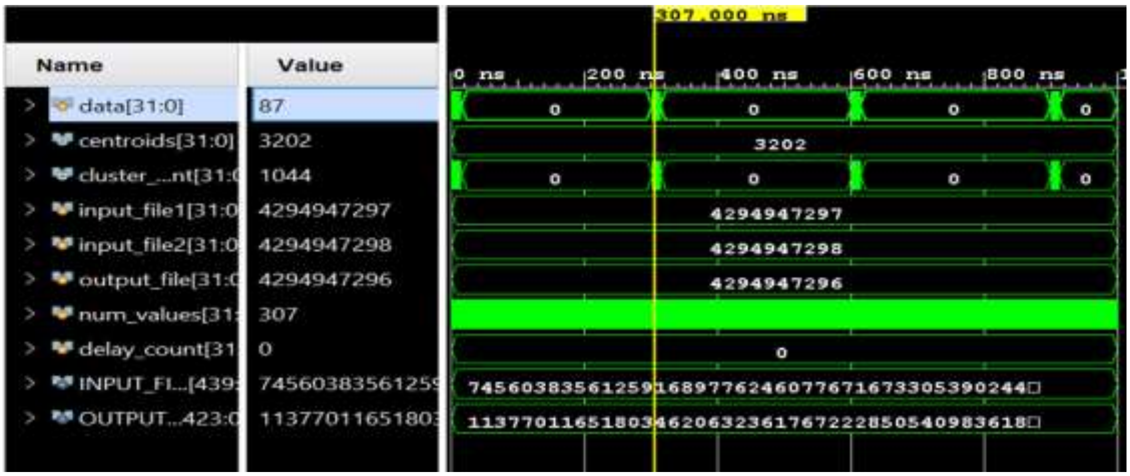

Figure 2. Simulation outcome

Resource	Utilization	Available	Utilization...
LUT	29	32600	0.09
IO	94	150	62.67

Figure 3. Design summary.

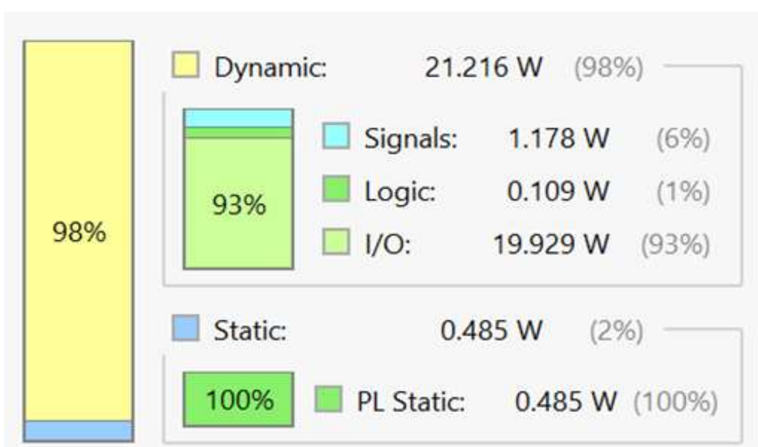

Figure 4. Power summary

Name	Slack ^1	Levels	Routes	High Fanout	From	To	Total Delay	Logic Delay	Net Delay	Requirement	Source Clock
Path 11	∞	4	2	3	data[7]	cluster_a...nment1[9]	3.689	1.498	2.191	-∞	input port clock
Path 12	∞	4	2	3	data[23]	cluster_as...ment1[25]	3.691	1.558	2.133	-∞	input port clock
Path 13	∞	4	2	3	data[4]	cluster_a...nment1[8]	3.711	1.516	2.195	-∞	input port clock
Path 14	∞	4	2	3	data[4]	cluster_a...nment1[6]	3.715	1.509	2.206	-∞	input port clock
Path 15	∞	3	2	3	data[6]	cluster_as...ment1[11]	3.725	1.519	2.206	-∞	input port clock
Path 16	∞	4	2	3	data[2]	cluster_a...nment1[4]	3.734	1.516	2.218	-∞	input port clock
Path 17	∞	4	2	3	data[8]	cluster_as...ment1[12]	3.735	1.508	2.227	-∞	input port clock
Path 18	∞	4	2	3	data[20]	cluster_as...ment1[24]	3.736	1.551	2.185	-∞	input port clock
Path 19	∞	3	2	3	data[10]	cluster_as...ment1[16]	3.741	1.580	2.161	-∞	input port clock
Path 20	∞	4	2	3	data[15]	cluster_as...ment1[17]	3.748	1.534	2.214	-∞	input port clock

Figure 5. Time summary

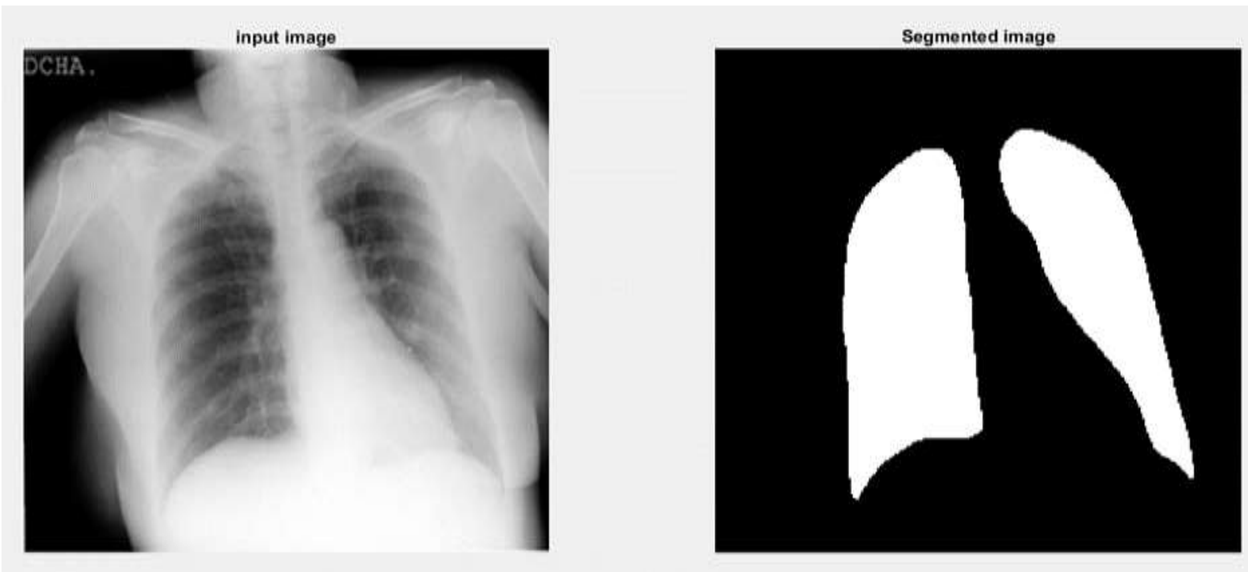

(a) (b)

Figure 6. Segmented Image Performance (a) Input Image (b) Proposed Segmented output image.

Table 1. Comparison Table

Parameter	Existing Method	Proposed Method
Accuracy	70.494	99.9959
Sensitivity	44.7561	99.9965
F-measure	50.8043	99.9921
Precision	61.3167	99.9877
MCC	30.0069	99.9893
Dice	50.8043	99.9921
Jaccard	38.8676	99.9842
Specificity	85.4226	99.9959

5. Conclusion

The VLSI implementation of chest X-ray image segmentation using hybrid clustering represents a significant advancement in medical imaging technology, poised to revolutionize diagnostic processes in healthcare. By combining the power of VLSI chips with innovative hybrid clustering techniques, this approach offers a promising solution for automatically segmenting chest X-ray images into meaningful regions for medical analysis. The integration of hybrid clustering algorithms, such as k-means, hierarchical clustering, and density-based clustering, allows for more accurate and robust segmentation, catering to the complex and variable characteristics of chest X-ray images. This groundbreaking implementation harnesses the parallel processing capabilities of VLSI chips to efficiently perform the computationally intensive tasks involved in image segmentation. By distributing the workload across multiple processing units on the VLSI chip, the segmentation process can be accelerated, enabling real-time or near-real-time analysis of chest X-ray images. This not only enhances the efficiency of medical diagnosis but also facilitates timely interventions and treatments for patients, potentially leading to improved patient outcomes and healthcare delivery.

References

[1]. Song, Jiang, Yuan Gu, and Ela Kumar. "Chest sdisease image classification based on spectral clustering algorithm." *Research Reports on Computer Science* (2023): 77-90.

[2]. Agrawal, Tarun, and Prakash Choudhary. "Segmentation and classification on chest radiography: a systematic survey." *The Visual Computer* 39, no. 3 (2023): 875-913.

[3]. Chakraborty, Gouri Shankar, Salil Batra, and Makul Mahajan. "A Novel Deep Learning-based Approach for Covid-19 Infection Identification in Chest X-ray Image using Improved Image Segmentation Technique." In *2023 7th International Conference on Trends in Electronics and Informatics (ICOEI)*, pp. 1102-1109. IEEE, 2023.

[4]. Lee, Beom J., Sarkis T. Martirosyan, Zaid Khan, Han Y. Chiu, Zun Wang, Wenqi Shi, Felipe Giuste, Yishan Zhong, Jimin Sun, and May Dongmei Wang. "Attention-based Automated Chest CT Image Segmentation Method of COVID-19 Lung Infection." In *2022 IEEE 22nd International Conference on Bioinformatics and Bioengineering (BIBE)*, pp. 158-163. IEEE, 2022.

[5]. Liu, Leon, and Yiqiao Yin. "Towards Explainable AI on Chest X-Ray Diagnosis Using Image Segmentation and CAM Visualization." In *Future of Information and Communication Conference*, pp. 659-675. Cham: Springer Nature Switzerland, 2023.

[6]. Wahyuningrum, Rima Tri, Indah Yunita, Indah Agustien Siradjuddin, Budi Dwi Satoto, Amillia Kartika Sari, and Anggraini Dwi Sensusiati. "Improvement of chest X-ray image segmentation accuracy based on FCA-Net." *Cogent Engineering* 10, no. 1 (2023): 2229571.

[7]. Gómez, Oscar, Pablo Mesejo, Oscar Ibáñez, Andrea Valsecchi, and Oscar Cordón. "Deep architectures for high-resolution multi-organ chest X-ray image segmentation." Neural Computing and Applications 32, no. 20 (2020): 15949-15963.

[8]. Gite, Shilpa, Abhinav Mishra, and Ketan Kotecha. "Enhanced lung image segmentation using deep learning." Neural Computing and Applications 35, no. 31 (2023): 22839-22853.

[9]. Iqbal, Ahmed, Muhammad Usman, and Zohair Ahmed. "Tuberculosis chest X-ray detection using CNN-based hybrid segmentation and classification approach." Biomedical Signal Processing and Control 84 (2023): 104667.

[10]. Jyoti, Kumari, Sai Sushma, Saurabh Yadav, Pawan Kumar, Ram Bilas Pachori, and Shaibal Mukherjee. "Automatic diagnosis of COVID-19 with MCA-inspired TQWT-based classification of chest X-ray images." Computers in Biology and Medicine 152 (2023): 106331.

[11]. Sulaiman, Adel, Vatsala Anand, Sheifali Gupta, Yousef Asiri, M. A. Elmagzoub, Mana Saleh Al Reshan, and Asadullah Shaikh. "A Convolutional Neural Network Architecture for Segmentation of Lung Diseases Using Chest X-ray Images." Diagnostics 13, no. 9 (2023): 1651.

[12]. Nayak, Soumya Ranjan, Janmenjoy Nayak, Utkarsh Sinha, Vaibhav Arora, Uttam Ghosh, and Suresh Chandra Satapathy. "An automated lightweight deep neural network for diagnosis of COVID-19 from chest X-ray images." Arabian journal for science and engineering 48, no. 8 (2023): 11085-11102.

[13]. Priya, R. Krishna, Ali Al Bimani, Mullaicharam Bhupathyraaj, Suhail Ahamed, Shyam Sundar Arputhanantham, and Susamma Chacko. "Fuzzy-entropic approach on chest X-ray region of interest segmentation-heart position shifting using differential evolution optimization and multi-level segmentation technique with cloud computing." Soft Computing 27, no. 3 (2023): 1639-1650.

[14]. Nawaz, Marriam, Tahira Nazir, Jamel Baili, Muhammad Attique Khan, Ye Jin Kim, and Jae-Hyuk Cha. "CXray-EffDet: chest disease detection and classification from X-ray images using the EfficientDet model." Diagnostics 13, no. 2 (2023): 248.

[15]. Shaheed, Kashif, Piotr Szczuko, Qaisar Abbas, Ayyaz Hussain, and Mubarak Albathan. "Computer-Aided Diagnosis of COVID-19 from Chest X-ray Images Using Hybrid-Features and Random Forest Classifier." In Healthcare, vol. 11, no. 6, p. 837. MDPI, 2023.

[16]. Srinivasarao, G., Penchaliah, U., Devadasu, G. et al. Deep learning based condition monitoring of road traffic for enhanced transportation routing. J Transp Secur 17, 8 (2024). https://doi.org/10.1007/s12198-023-00271-3

[17]. Arvind, S., Jitendra V. Tembhurne, Tausif Diwan, and Parul Sahare. "Improvised light weight deep CNN based U-Net for the semantic segmentation of lungs from chest X-rays." Results in Engineering 17 (2023): 100929.

[18]. Rajaraman, Sivaramakrishnan, Feng Yang, Ghada Zamzmi, Zhiyun Xue, and Sameer Antani. "Assessing the Impact of Image Resolution on Deep Learning for TB Lesion Segmentation on Frontal Chest X-rays." Diagnostics 13, no. 4 (2023): 747.

[19]. dos Santos Silva, Bruno Riccelli, Paulo Cesar Cortez, Rafael Gomes Aguiar, Tulio Rodrigues Ribeiro, Alexandre Pereira Teixeira, Francisco Nauber Bernardo Gois, and Joao Alexandre Lobo Marques. "Lung Segmentation of Chest X-Rays Using Unet Convolutional Networks." In Computerized Systems for Diagnosis and Treatment of COVID-19, pp. 15-28. Cham: Springer International Publishing, 2023.

[20]. Rollan-Martinez-Herrera, Maria, Jagoba Zuluaga-Ayesta, Francisco Martinez-Dubarbie, Marta Garrido-Barbero, Ane Zubizarreta-Zamalloa, and Raul San José Estépar. "Thorax-Net: A Full Thoracic Chest X-Ray Segmentation Approach." In International KES Conference on Innovation in Medicine and Healthcare, pp. 385-393. Singapore: Springer Nature Singapore, 2023.

[21]. Farhan, Abobaker Mohammed Qasem, and Shangming Yang. "Automatic lung disease classification from the chest X-ray images using hybrid deep learning algorithm." Multimedia Tools and Applications (2023): 1-27.